Ultrashort electron beam generation from resonantly excited nonlinear laser wakefield

K. Nagashima, Y. Kishimoto, and H. Takuma
Advanced Photon Research Center, Japan Atomic Energy Research Institute, Tokai-mura, Naka-gun, Ibaraki-ken 319-1195, Japan
(Recieved 28 September 1998)

A method for generating an ultrashort electron beam from a resonantly excited nonlinear wake field is proposed using a short laser pulse with a relativistic intensity. The considerable amount of electrons up to 10 C/m^2 are extracted from an appropriate thin plasma layer. When the laser intensity is highly relativistic, the electron beam is singly bunched and has a pulse length less than the laser wavelength and a large energy spread with a maximum energy of tens of MeV. [S1063-651X(99)11901-9]

PACS number(s): 41.75.Ht, 52.40.Nk, 52.60.+h, 52.65.Rr

Recent advances in laser technology have made plasma-based particle accelerators attractive [1–5]. The relativistic laser wake field is of current interest in this context [6]. In the experiments on laser acceleration [2–5], intense short pulse lasers are focused in underdense plasma and longitudinal plasma waves are excited with the phase velocity close to the speed of light. Electron beams with relativistic velocity are injected on the same axis with the laser beams and electrons are accelerated in the accelerating phase of the plasma waves. Therefore, in this technique, a short pulse bunched electron beam is suitable as the injection beam and it is convenient to generate this electron beam also using laser pulses in order to construct a compact device. In the experiments using the self-modulated laser wake field, background plasma electrons are accelerated up to highly relativistic energy [7–10]. It is suggested that the production of high-energy electrons is caused by stimulated Raman scattering [11]. The observed electrons show large shot-to-shot fluctuations because of the strong nonlinearity of the laser-plasma interaction [10]. Recently, the characteristics of the generated electron beam have been examined in detail and found to have a continuous energy spread with a maximum energy above tens of MeV [12]. In this case using the self-modulated laser wake field, the electrons are multibunched with the spatial interval of the plasma wavelength. The total pulse length of the electron beam is approximately equal to that of the laser pulse. In this paper, we propose a method for generating an ultrashort bunched electron beam from a resonantly excited nonlinear laser wake field using a shorter laser pulse with a highly relativistic intensity.

The nonlinear wake field was extensively studied by relativistic electron fluid equations [6] and particle-in-cell (PIC) simulations [13]. A characteristic parameter of the intense laser field is the normalized field amplitude, $a_0 = eE_0/m_e\omega_0 c$, where E_0 is the laser electric field and ω_0 is the laser angular frequency. The electron quiver motion is relativistic when $a_0 > 1$. When the laser pulse length is approximately equal to a half of the plasma wavelength, $c\tau_{\mathrm{FWHM}} \approx \lambda_p/2$ (where FWHM is full width at half-maximum), the wake field is excited resonantly [where the plasma wavelength is $\lambda_p = 2\pi c/\omega_p$ and the plasma frequency is $\omega_p = (n_e e^2/m_e\epsilon_0)^{0.5}$]. At the relativistic laser intensity, the excited plasma wave is steepened nonlinearly [6] and produces high-energy electrons directed to the laser propagating direction [13]. In this case, the generated high-energy electrons are bunched in the longitudinal direction. It is supposed that the electron beam can be extracted from the plasma region, when a plasma-vacuum boundary is formed in the plane normal to the laser propagating direction.

Here, the characteristics of the extracted electron beam are examined using one-dimensional 1D and 2D PIC simulations. These are self-consistent electromagnetic relativistic codes with mobile ions. The numerical algorithm used in the codes is following to that in Ref. [14]. In our simulations, the laser pulse has a wavelength $\lambda_0 = 800$ nm, a pulse length $\tau_{\mathrm{pulse}} = 16$ fs (a full width at e^{-1} of the electric field), a peak intensity $I_0 = 10^{18} - 10^{20}$ W/cm^2 ($a_0 = 0.68 - 6.8$) and a linear polarization. The pulse shape is assumed to be Gaussian in both longitudinal and transverse directions. A 2000×500 Cartesian mesh is used in an x-y simulation plane with a spatial mesh size of $0.1\lambda_0$. The laser pulse propagates in the x direction and is polarized in the z direction. The laser pulse is focused at the center in the x direction and the focal spot diameter, which is defined as a full width at e^{-1} of the electric field, is $12\lambda_0$ in 2D simulations. The plasma consists of electrons and ions with an ion mass of $m_i = 1836 m_e$. Initially, the particles are placed in a central region of the x direction with an uniform or triangular profile. The plasma layer ($-w/2 \leqslant x \leqslant w/2$, w is the width of the initial plasma region) is bounded by two vacuum regions in the x direction.

The nonlinear wake field is affected by a wave breaking process [15,16]. The condition of the wave breaking is given by $E_x \approx \alpha m_e \omega_p c/e$ approximately, where α is a value of the order of unity. Using the phase velocity of the wake field, $v_{\mathrm{ph}}/c = 0.95 - 0.99$ [17], the value of α is estimated to be 2–3 for cold plasma [16]. As the maximum amplitude of the wake field is given by [6]

$$E_{\max} = \frac{m_e \omega_0 c}{e} \frac{a_0^2}{\sqrt{1+a_0^2}}, \tag{1}$$

the wave breaking affects the wake field and produces high-energy electrons for $a_0 \geqslant 2-3$. In the result of PIC simulations [12], the wave breaking occurs at $\alpha = 1.8$. However, the authors commented that they found no general rule for estimating the wave amplitude at wave breaking. Once the wave breaking occurs, the wake field is decayed during a few times ω_p^{-1} [13]. In more highly relativistic case, the wake field is decayed during less than ω_p^{-1} and the wave with only

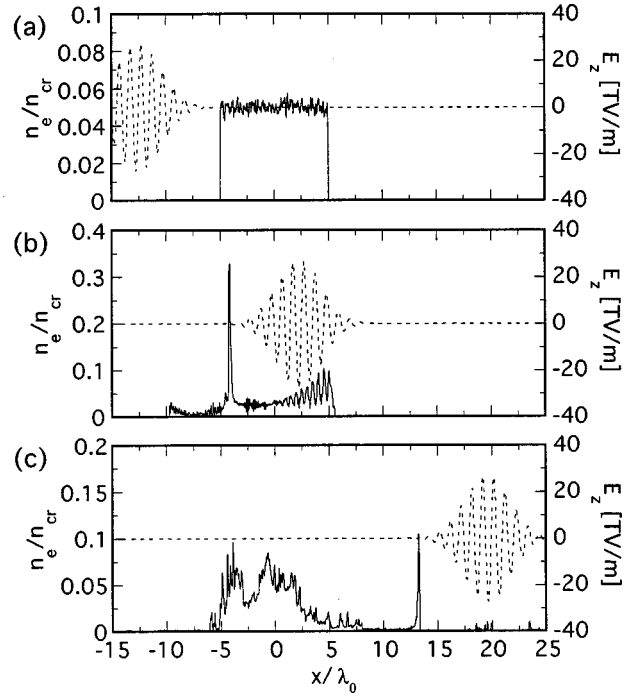

FIG. 1. Electron density profiles following the laser pulse propagation in the 1D simulation for a peak laser intensity of $I_0 = 10^{20}$ W/cm^2 and a flat initial density profile with $n_e/n_{cr} = 0.05$. The peak of envelope of the laser field is located at $x/\lambda_0 = -12.5$ (a), $x/\lambda_0 = 2.5$ (b), and $x/\lambda_0 = 20$ (c).

single cycle survives. Therefore, in this case, it is expected that singly bunched electron beam is generated.

Figure 1 shows electron density profiles following the laser pulse propagation in the 1D simulation for the peak laser intensity of $I_0 = 10^{20}$ W/cm^2 ($a_0 = 6.8$) and the flat initial density profile with $n_e/n_{cr} = 0.05$ [Fig. 1(a)], where n_{cr} is the critical density. When the laser pulse penetrates into the plasma, a strongly bunched electron beam is generated [Fig. 1(b)]. After the laser pulse passing the plasma region, the electron beam is extracted from this region [Fig. 1(c)]. This single electron beam has an ultrashort pulse length less than the laser wavelength and an appropriate delay from the laser field. This delay is important because the extracted electron beam is not disturbed by the laser field. In this case, the resonance condition of the wake field is obtained as $n_e/n_{cr} \approx 0.02$. As shown in Fig. 1(b), the initial density profile is disturbed by the laser pulse and the electron density decreases in an area where the wake field is excited. Therefore, the resonance condition is approximately satisfied in spite of the high initial electron density. In the two-dimensional case, this effect is enhanced by the transverse ponderomotive force.

The extracted electron charge depends on the laser intensity, the width of the plasma region, and the electron density. The dependence has been examined by 1D simulations. For the excitation of the wake field, the width of the plasma region must be wider than the plasma wavelength, $w > \lambda_p$. Figure 2(a) shows the dependence of the extracted charge on the width of the plasma region with the initial electron density of $n_e/n_{cr} = 0.02$. The charge was calculated from the electrons in the region of $x \geqslant w/2 + 15\lambda_0$ when the peak of the laser pulse propagated up to $x = w/2 + 35\lambda_0$. The plasma

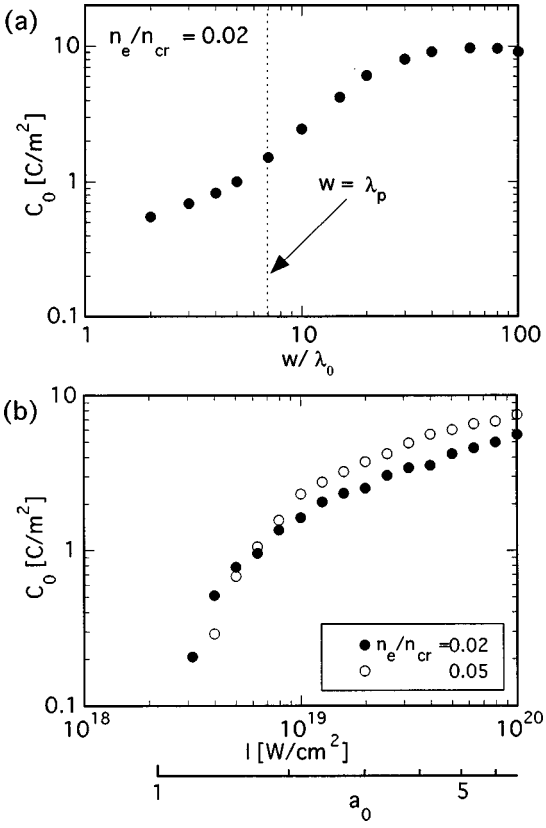

FIG. 2. Dependence of the extracted electron charge on the width of the plasma region (a) and the laser intensity (b). The other parameters are fixed at a laser intensity of $I_0 = 10^{20}$ W/cm^2, the width of the plasma region of $20\lambda_0$ and the initial electron density of $n_e/n_{cr} = 0.02, 0.05$.

wavelength is $\lambda_p/\lambda_0 \approx 7$ for the initial electron density. The charge is saturated in the range of $w/\lambda_p \geqslant 3$. In the shown cases with $w/\lambda_0 \leqslant 100$, the absorption of the laser energy is not so significant. But, for higher density and/or wider plasma region, the absorption is significant and the extracted charge decreases. The extracted charge depends on the laser

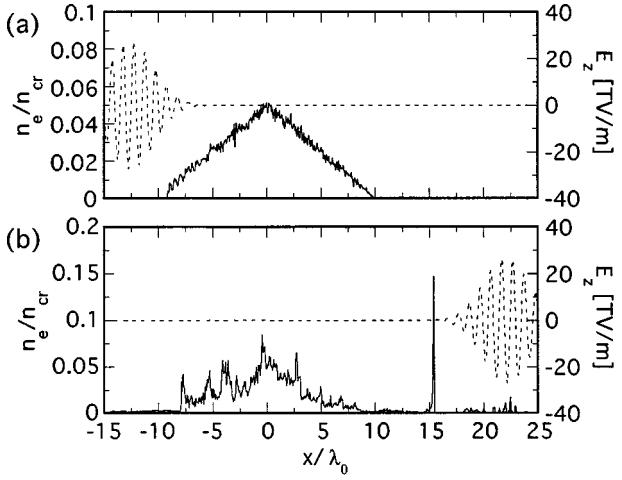

FIG. 3. Electron density profiles for the triangular initial density profile. The simulation parameters are the same as those in Fig. 1, except for the initial density profile. The peak of envelope of the laser field is located at $x/\lambda_0 = -12.5$ (a) and $x/\lambda_0 = 22.5$ (b).

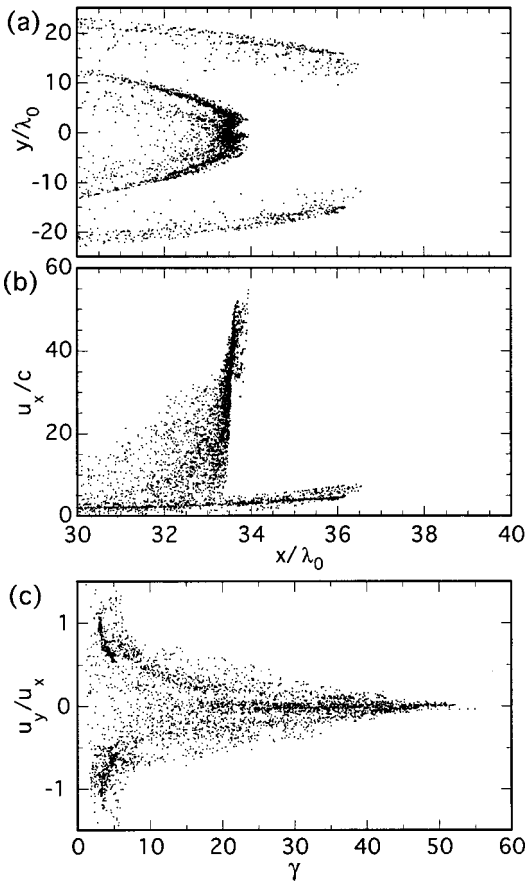

FIG. 4. Distributions of the extracted electrons in the x-y space (a), in the x-u_x space (b), and in the γ-u_y/u_x space (c) for the 2D simulation with a peak laser intensity of $I_0=10^{20}$ W/cm^2, a width of the plasma region of $20\lambda_0$, and an initial electron density of $n_e/n_{cr}=0.05$.

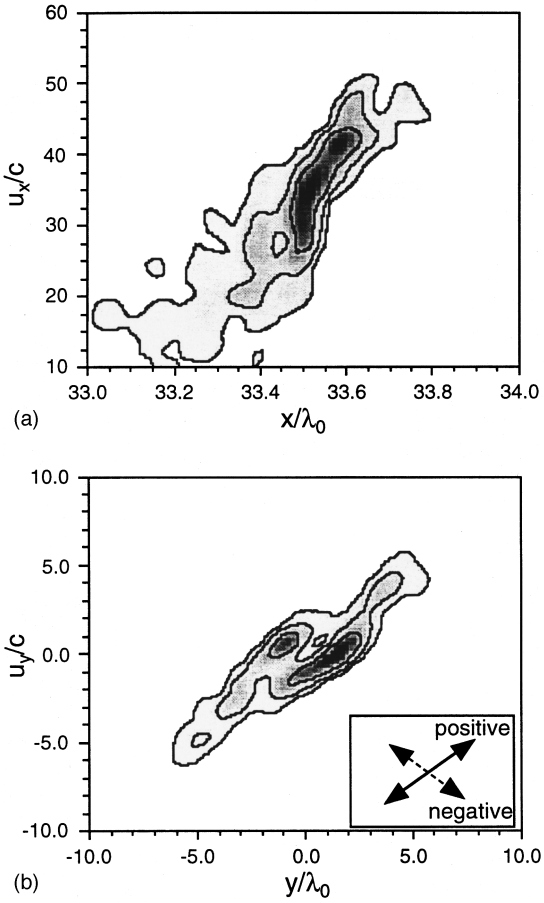

FIG. 5. Contour plots of electron densities in the phase spaces of x-u_x (a) and y-u_y (b). There are three contour lines, which are $\frac{1}{2}$, $\frac{1}{4}$, and $\frac{1}{10}$ of the maximum values.

intensity. Figure 2(b) shows the dependence for two cases with electron densities of $n_e/n_{cr}=0.02$ and 0.05. The width of the plasma region is $20\lambda_0$ in the both cases. The electrons are extracted for $a_0>1$ as can be estimated from the nonlinear feature of the wakefield. The extracted charge increases with increasing the laser intensity, but the dependence is weak in the high-intensity range. Since the extracted charge has no strong dependence on the electron density, no fine control of the resonance condition is needed for extracting the electron beam.

The initial density profile affects the extraction of the electron beam. In real situations, the density profiles have finite gradients in plasma-vacuum boundaries. This effect has been examined using a triangular profile as shown in Fig. 3(a). The peak density and the total number of electrons are equal to those in Fig. 1 (the width of the plasma region is twice that of Fig. 1 and the average density is a half). In this case, the extracted charge [Fig. 3(b)] is not so different from that shown in Fig. 1(c). For a trapezoidal density profile, if the density scale length in the boundary region was $\leqslant\lambda_p$, the extracted charge was nearly equal to that for the flat profile. However, we have found no general dependence on the density profiles.

The characteristics of the extracted electron beam have been examined from 2D simulations. Figure 4(a) shows a plot of the extracted electrons in the x-y plane for the simulation with a peak laser intensity of $I_0=10^{20}$ W/cm^2, a width of the plasma region of $w/\lambda_0=20$ ($-10\leqslant x/\lambda_0\leqslant 10$), and an electron density of $n_e/n_{cr}=0.05$. There are two groups of electrons; one is located in the central region of $|y/\lambda_0|\leqslant 12$ (group 1) and the other in the peripheral region of $|y/\lambda_0|\geqslant 12$ (group 2). The electrons in group 1 are generated by the wake field and those in group 2 are generated by the ponderomotive and $v\times B$ forces of the laser field. Figure 4(b) is a distribution of the electrons in the phase space of x-u_x, where u_x is defined as $u_x=\gamma v_x=p_x/m_e$ (v_x, p_x, and γ are the normal velocity, the momentum, and the relativistic factor, respectively) and u_x/c is the normalized momentum. The electrons in group 1 have large momentum up to a maximum of $u_x/c\approx 50$, which is quite a bit larger than the quivering momentum of $a_0=6.8$. The electrons in group 2 have smaller momentum of $u_x/c\leqslant 7$. These two groups of electrons have quite different directions of the momentum in the x-y plane. Figure 4(c) shows a distribution of the ratio u_y/u_x as a function of the relativistic factor. The electrons in group 1 have small values and the beam divergence is small. But the electrons in group 2 have large values in the range of $u_y/u_x=0.5-1$. This large transverse momentum is given by the transverse ponderomotive force in the laser field.

We have examined the beam characteristics of electrons in group 1, which are located in the region of $33\leqslant x/\lambda_0\leqslant 34$ and $-10\leqslant y/\lambda_0\leqslant 10$. Figure 5 shows contour plots of

electron densities in the phase spaces of x-u_x and y-u_y. There are three contour lines, which are $\frac{1}{2}$, $\frac{1}{4}$, and $\frac{1}{10}$ of the maximum values. In Fig. 5(a), the full widths of the half maximum are $\Delta x/\lambda_0 \approx 0.1$ and $\Delta u_x/c \approx 15$. Therefore, this beam has a very small spatial spread in the longitudinal direction and a large energy spread with a maximum energy of 25 MeV. The spread in the y-u_y phase space [Fig. 5(b)] is rather complicated. There are two kinds of split of the beam, one is the split in the positive direction and the other in the negative direction [the two directions are indicated in the small window of Fig. 5(b)]. The positive split is caused by the Coulomb force and/or the transverse ponderomotive force of the laser field. It has been found that the negative split is originated from the spatial distribution of the wake field. The spread in the y-u_y space depends on the plasma parameters, especially the electron density and the profile shape. In the simulation with the density of $n_e/n_{cr}=0.02$ and the other parameters the same as those in Fig. 4, the spread in the y-u_y space is significantly large. So, the beam emittance is complicatedly dependent on the simulation parameters.

In conclusion, we have proposed a method for generating an ultrashort electron beam from a resonantly excited nonlinear wake field using a short laser pulse with relativistic intensity. The electrons up to 10 C/m^2 are extracted from the thin plasma layer with a width of $w/\lambda_0 \approx 10-100$. The extracted charge is 1 nC for the focal spot diameter of 10 μm. When the laser intensity is highly relativistic, the electron beam is singly bunched and has a pulse length less than the laser wavelength. The characteristics of the extracted electron beam have been examined in detail from the 2D simulations. The beam has a large energy spread with a maximum energy of tens of MeV. Although the spatial spread in the longitudinal direction is very small, the spread in the transverse direction is complicatedly dependent on plasma parameters.

It is pleasure to acknowledge the support of the staff at the Advanced Photon Research Center. The authors would like to thank Dr. T. Tajima for his many helpful comments.

[1] T. Tajima and J. M. Dawson, Phys. Rev. Lett. **43**, 267 (1979).
[2] C. E. Clayton *et al.*, Phys. Rev. Lett. **70**, 37 (1993).
[3] F. Amiranoff *et al.*, Phys. Rev. Lett. **74**, 5220 (1995).
[4] K. Nakajima *et al.*, Phys. Rev. Lett. **74**, 4428 (1995).
[5] D. Umstadter *et al.*, Science **273**, 472 (1996).
[6] P. Sprangle, E. Esarey, and A. Ting, Phys. Rev. Lett. **64**, 2011 (1990); P. Sprangle, E. Esarey, and A. Ting, Phys. Rev. A **41**, 4463 (1990); A. Ting, E. Esarey, and P. Sprangle, Phys. Fluids B **2**, 1390 (1990).
[7] C. A. Coverdale *et al.*, Phys. Rev. Lett. **74**, 4659 (1995).
[8] A. Modena *et al.*, Nature (London) **337**, 606 (1995).
[9] R. Wagner, S.-Y. Chen, A. Maksimchuk, and D. Umstadter, Phys. Rev. Lett. **78**, 3125 (1997).
[10] C. I. Moore *et al.*, Phys. Rev. Lett. **79**, 3909 (1997).
[11] C. D. Decker, W. B. Mori, and T. Katsouleas, Phys. Rev. E **50**, R3338 (1994).
[12] K.-C. Tzeng, W. B. Mori, and T. Katsouleas, Phys. Rev. Lett. **79**, 5258 (1997).
[13] S. V. Bulanov, F. Pegoraro, and A. M. Pukhov, Phys. Rev. Lett. **74**, 710 (1995).
[14] C. K. Birdsall and A. B. Langdon, in *Plasma Physics via Computer Simulation* (McGraw-Hill Book Company, 1985), p. 351.
[15] A. I. Akhiezer and R. V. Polovin, Zh. Eksp. Teor. Fiz. **30**, 915 (1956) [Sov. Phys. JETP **3**, 696 (1956)]; J. M. Dawson, Phys. Rev. **113**, 383 (1959).
[16] Z. M. Sheng and J. Meyer-ter-Vehn, Phys. Plasmas **4**, 493 (1997).
[17] C. D. Decker and W. B. Mori, Phys. Rev. Lett. **72**, 490 (1994).